

# *Plasmodium falciparum* Histones Induce Endothelial Proinflammatory Response and Barrier Dysfunction

Mark R. Gillrie,\* Kristine Lee,\* D. Channe Gowda,<sup>†</sup> Shevaun P. Davis,\* Marc Monestier,<sup>‡</sup> Liwang Cui,<sup>§</sup> Tran Tinh Hien,<sup>¶</sup> Nicholas P.J. Day,<sup>¶</sup> and May Ho\*

From the Department of Microbiology Immunology & Infectious Diseases,\* University of Calgary, Alberta, Canada; the Department of Biochemistry and Molecular Biology,<sup>†</sup> Pennsylvania State University College of Medicine, Hershey, Pennsylvania; the Temple Autoimmunity Center,<sup>‡</sup> Department of Microbiology and Immunology, Temple University School of Medicine, Philadelphia, Pennsylvania; the Department of Entomology,<sup>§</sup> Pennsylvania State University, University Park, Pennsylvania; and the Oxford University Clinical Research Unit,<sup>¶</sup> Hospital for Tropical Diseases, Ho Chi Minh City, Vietnam

***Plasmodium falciparum* is a protozoan parasite of human erythrocytes that causes the most severe form of malaria. Severe *P. falciparum* infection is associated with endothelial activation and permeability, which are important determinants of the outcome of the infection. How endothelial cells become activated is not fully understood, particularly with regard to the effects of parasite subcomponents. We demonstrated that *P. falciparum* histones extracted from merozoites (HeH) directly stimulated the production of IL-8 and other inflammatory mediators by primary human dermal microvascular endothelial cells through a signaling pathway that involves Src family kinases and p38 MAPK. The stimulatory effect of HeH and recombinant *P. falciparum* H3 (PfH3) was abrogated by histone-specific antibodies. The release of nuclear contents on rupture of infected erythrocytes was captured by live cell imaging and confirmed by detecting nucleosomes in the supernatants of parasite cultures. HeH and recombinant parasite histones also induced endothelial permeability through a charge-dependent mechanism that resulted in disruption of junctional protein expression and cell death. Recombinant human activated protein C cleaved HeH and PfH3 and abrogated their proinflammatory effects. Circulating nucleosomes of both human and parasite origin were detected in the plasma of patients with falciparum malaria and correlated positively with disease severity. These results support a pathogenic role for both host-**

**and pathogen-derived histones in *P. falciparum*-caused malaria. (Am J Pathol 2012, 180:1028–1039; DOI: 10.1016/j.ajpath.2011.11.037)**

*Plasmodium falciparum*, the causative agent of the most severe form of malaria, is a protozoan parasite of human erythrocytes. Because of their intravascular localization, *P. falciparum*-infected erythrocytes (IRBCs) are in intimate contact with vascular endothelium throughout the 48 hours of the parasite life cycle, particularly in the second half of the life cycle, when mature parasites adhere to the endothelium by means of parasite proteins that are transported to the IRBC surface.<sup>1</sup> Cytoadherence is vital to the survival of the parasites, in that it allows them to evade clearance by the spleen. Unfortunately, the process may also lead to pathology in the host through obstruction of microcirculatory blood flow, with resulting tissue hypoxia, metabolic disturbances, and organ dysfunction.<sup>2</sup>

A further consequence of cytoadherence is the release of parasite products or components in close proximity to the endothelium at the time of schizogony. Several released components have been shown to induce a proinflammatory response in different immune cell types. For example, the glycosylphosphoinositol (GPI) anchor of malarial cell surface proteins on plasma membranes stimulates TNF- $\alpha$  and IL-12 production by macrophages.<sup>3–6</sup> Hemozoin (Hz), a polymer of heme that accumulates in the digestive vacuole of intraerythrocytic parasites as an insoluble by-product of hemoglobin degradation, or a synthetic preparation from hemin, activates the NOD-like receptor containing pyrin domain 3 (NLRP3) inflammasome in lipopolysaccharide-primed macrophages.<sup>7–9</sup> As well, Hz has been reported to function as

Supported by a Canadian Institutes of Health Research (CIHR) grant MT14104 (M.H.). M.H. is a Scientist of Alberta Innovates-Research Solutions, Canada. M.R.G. is supported by an M.D./Ph.D. scholarship from CIHR.

Accepted for publication November 4, 2011.

Supplemental material for this article can be found at <http://ajp.amjpathol.org> or at doi: 10.1016/j.ajpath.2011.11.037.

Address reprint requests to May Ho, M.D., Department of Microbiology and Infectious Diseases, 3330 Hospital Dr. NW, Calgary, AB, Canada T2N 4N1. E-mail: [mho@ucalgary.ca](mailto:mho@ucalgary.ca).

a carrier of malarial DNA into mouse bone marrow-derived dendritic cells for the recognition of DNA by TLR9,<sup>10</sup> or to activate TLR9 directly.<sup>11</sup> Most recently, the TLR9-dependent proinflammatory effect of plasmodial components on human plasmacytoid dendritic cells was found to be induced by nucleosomes<sup>12</sup> in which the histones are believed to provide a positive charge that facilitates internalization of parasite DNA, analogous to the role of the antimicrobial cationic peptide LL37 in shuttling host DNA into plasmacytoid dendritic cells in psoriasis.<sup>13</sup> *P. falciparum* also produces uric acid,<sup>14</sup> a metabolite that has the potential to activate the NLRP3 inflammasome.<sup>15</sup> Endogenous uric acid could also be released from host cells damaged by Hz.<sup>14,16</sup>

Compared with the extensive investigations with classical antigen-presenting cells, the interaction between *P. falciparum* components and microvascular endothelium is less well studied. Endothelial cells may in fact have a critical role in host response to microbial pathogens, in terms of protection, pathogenesis, or both.<sup>17–19</sup> For patients who have died from severe falciparum malaria, there is histopathological evidence from both adult and pediatric patient populations of widespread endothelial activation that is manifested as up-regulation of adhesion molecule expression, chemokine/cytokine production, and endothelial permeability.<sup>20,21</sup> Clinically, disruption of blood-brain barrier integrity is associated with cerebral malaria, the complication that predominates in children,<sup>22</sup> and vascular leakage and leukocyte recruitment are hallmarks of the acute lung injury syndrome seen in adults.<sup>23,24</sup> Whether endothelial activation occurs as a response to leukocyte-derived proinflammatory mediators or as a direct response to parasites is not well documented. In particular, few studies have addressed the role of specific subcellular parasite components on endothelial cell dysfunction. We have previously reported that endothelial permeability in primary dermal and lung microvascular endothelium *in vitro* could be induced by *P. falciparum* merozoite proteins by disruption of junctional protein expression through a Src family kinase-mediated mechanism.<sup>25</sup>

Histones are small, detergent-insoluble, acid-soluble proteins found abundantly in insoluble chromatin complexes. Until recently, histones have been thought of primarily as a key component of chromatin, regulating gene transcription. There is now growing evidence to support important extrachromatin functions of histones in infections. Histones may have potent antimicrobial effect through induction of pore formation in bacterial cell membranes as a result of their positive charge.<sup>26</sup> As well, granulocytes (primarily neutrophils) can extrude histone-rich chromatin to generate neutrophil extracellular traps that capture and kill bacteria.<sup>25,27</sup> On the other hand, extracellular histones have been demonstrated to mediate endothelial cytotoxicity, leading to gross morphological changes associated with acute lung injury in mice *in vivo* and in human endothelial cells *in vitro*.<sup>28</sup> Moreover, anti-histone antibodies dramatically reduced mortality in several murine models of severe sepsis. Because nuclear proteins are highly conserved, we hypothesized that plasmodial histones from merozoites may have a

similar role in the induction of endothelial dysfunction in severe falciparum malaria.

In the present study, we investigated the role of *P. falciparum* histones on the induction of IL-8 and endothelial barrier dysfunction in primary microvascular endothelial cells *in vitro*. We found that *P. falciparum* histones induce both a proinflammatory response and endothelial permeability in primary human dermal and lung microvascular endothelial cells. Parasite histones also increased endothelial permeability by inducing disruption of junctional proteins and cell death, which may be related to the high positive charge on these nuclear proteins. Both IL-8 induction and permeability were inhibited by recombinant human activated protein C (rhAPC) that cleaved plasmodial histones. The release of nuclear contents on IRBC rupture was captured by live cell imaging and was confirmed by the detection of nucleosomes in supernatants of parasite cultures. Circulating nucleosomes of human and parasite origin were detected in the plasma of patients with falciparum malaria and correlated positively with severity. Taken together, our results suggest that extracellular histones may have an important role in the pathogenesis of severe falciparum malaria.

## Materials and Methods

### Tissue Culture and Other Reagents

Unless otherwise stated, all tissue culture reagents were purchased from Invitrogen Canada (Burlington, ON, Canada) and chemical reagents were purchased from Sigma-Aldrich (Oakville, ON, Canada). The Src-family kinase inhibitor PP1 and the inactive analog PP3 were purchased from Enzo Life Sciences International (Plymouth Meeting, PA). ZVAD-fmk was purchased from Calbiochem (EMD4BioSciences, San Diego, CA). Chemiluminescence horseradish peroxidase substrate was purchased from Millipore (Billerica, MA). The substrate 3,3',5,5'-tetramethylbenzidine (Pierce TMB) was purchased from Thermo Scientific (Rockford, IL). Recombinant human histone H4 was purchased from New England Biolabs (Ipswich, MA). DNase I was purchased from Qiagen Canada (Mississauga, ON, Canada). Recombinant human activated protein C [drotrecogin alfa (activated)] was a kind gift of Dr. Brent Winston, Department of Critical Care, Foothills Hospital, Calgary, AB, Canada.

### Parasites and Patient Plasma

The laboratory-adapted parasite clone 3D7 was cultured at 37°C and 5% CO<sub>2</sub> for histone extraction from merozoites. The stock parasites were shown to be mycoplasma-free by real-time quantitative PCR (qPCR) (Stratagene, La Jolla, CA). Aliquots of parasites were cultured for a maximum of 2 weeks. Plasma samples from a large study of adult patients with severe falciparum malaria<sup>29,30</sup> were obtained from the Center for Tropical Diseases, Ho Chi Minh City, Vietnam. The collection of clinical specimens was approved by the Ethics and Scientific Committee of the Center for Tropical Diseases. Informed consent was

obtained from all patients and/or relatives according to the Declaration of Helsinki.

### Antibodies

Polyclonal antibody to human ZO-1 was purchased from Zymed (Invitrogen). Fluorescein isothiocyanate (FITC) or Alexa Fluor 488 labeled anti-rabbit secondary antibodies were purchased from Molecular Probes (Invitrogen). Anti-His-probe antibodies were purchased from Santa Cruz Biotechnology (Santa Cruz, CA). Anti-p38 MAPK and anti-phospho-Thr 180/Tyr182 p38 MAPK were purchased from Cell Signaling Technology (Danvers, MA). Anti-phospho-Tyr 418 Src was purchased from BioSource (Invitrogen). Anti-TLR2 (clone 2.5), anti-hTLR4-IgA (clone W7C11), and control IgA2 (clone T9C6) were purchased from InvivoGen (San Diego, CA). Mouse IgG1 (clone 11711) was purchased from R&D Systems (Minneapolis, MN). Horseradish peroxidase-conjugated secondary antibodies were purchased from Jackson ImmunoResearch Laboratories (West Grove, PA). Monoclonal antibodies to mouse H3 (LG2-1) and H2A/H4 (BWA3) were produced as described previously.<sup>31</sup>

### Endothelial Cells

Human dermal microvascular endothelial cells (HDMECs) were harvested from discarded neonatal human foreskins using 0.5 mg/mL Type IA collagenase (Roche Diagnostics, Indianapolis, IN) as described previously.<sup>32</sup> The collection of skin specimens for isolation of endothelial cells was approved by the Conjoint Ethics Board of Alberta Health Services and the University of Calgary, Alberta, Canada. The cells were maintained in endothelial basal medium (EBM; Lonza Walkersville, Walkersville, MD), with supplements provided by the manufacturer. Experiments were performed with cells from passages one to five that showed consistent response in Transwell permeability assays (see below). Primary human blood lung microvascular endothelial cells at passage 3 were purchased from Lonza and maintained in the same medium as HDMECs. Lung cells were used from passage four to eight.

### Purification of Parasite Histones

*P. falciparum* histones were purified from merozoites as described previously.<sup>33</sup> Briefly, released merozoites of 3D7 parasites at schizogony were extracted in 25 mmol/L Tris-HCl (pH 7.8) containing 1 mmol/L EDTA and 0.2% (v/v) Nonidet P40 (NP40). Extracts were washed in 0.8 mol/L NaCl followed by incubation with 10 volumes of 0.25 mol/L HCl on ice for 1 hour with constant mixing. Acid-insoluble contaminants including all hemozoin were pelleted. The HCl extract was neutralized to pH 7 by adding NaOH, and double-distilled water was added to return salt concentrations to physiological levels (0.9%). Preparations were concentrated using 3-kDa centrifuge filters (Millipore). The supernatant was analyzed by SDS-PAGE or frozen in aliquots at  $-80^{\circ}\text{C}$ . Protein levels of supernatants were quantified by a Bradford protein assay

(Bio-Rad Laboratories, Mississauga, ON, Canada). DNA content was determined by a Quant-iT PicoGreen double-stranded DNA kit (Molecular Probes, Invitrogen). Endotoxin content was determined by a PyroGene recombinant factor C kit (Lonza).

### Recombinant Histone Preparation

Recombinant H3 from *P. falciparum* (PfH3) was prepared as described previously.<sup>34</sup> Recombinant PfH3 pET22(b)<sup>+</sup> plasmid was expressed in *Escherichia coli* strain BL21 (DE3) (Invitrogen) with 1 mmol/L isopropyl- $\beta$ -D-thiogalactopyranoside induction for 5 hours at  $30^{\circ}\text{C}$ . His-tagged protein was purified by Talon beads (Clontech Laboratories, Mountain View, CA) under denaturing conditions with the addition of 8 mol/L urea. After purification, the recombinant proteins were eluted with imidazole and re-natured by extensive dialysis with gradually reduced urea concentrations, and finally with PBS at  $4^{\circ}\text{C}$ . Insoluble proteins were further removed by centrifugation at  $10,000 \times g$  for 10 minutes. The presence of endotoxin was determined by means of a PyroGene recombinant factor C kit (Lonza).

### Live Cell Imaging of IRBC Rupture

Live cell imaging was performed in an ibidi  $\mu$ -slide VI<sup>0.4</sup> chamber (ibidi GmbH, Munich, Germany) equilibrated and maintained at  $37^{\circ}\text{C}$  and 5%  $\text{CO}_2$  for the duration of the experiment. Late-stage ( $\sim 46$  hours) IRBCs were purified to  $>99\%$  using magnetic-activated cell sorting (MACS LS; Miltenyi Biotec, Auburn, CA) columns as described previously.<sup>35</sup> Purified IRBCs were washed twice with RPMI 1640 medium and added to ibidi chambers precoated with poly-L-lysine (1  $\mu\text{mol/L}$  for 10 minutes) to immobilize IRBCs for prolonged imaging. Nonadherent IRBCs were washed off with RPMI 1640, after which RPMI 1640 with 0.5% Albumax and 300 nmol/L Sytox Green was added to the chambers for the remainder of the experiment. IRBCs were imaged using an Olympus IX81 inverted confocal microscope (Olympus America, Center Valley, PA) with a PlanAPO 60 $\times$  oil immersion objective (NA 1.42) and were controlled and captured with Olympus FluoView 1000 software. Images were captured at 0 and 4 hours. Serial images of the same field of view were also acquired over the course of 10 minutes, showing rupture of a schizont and a merozoite. These still images were compiled into a video with ImageJ software version 1.44 (NIH, Bethesda, MD) and Microsoft Windows Live Movie Maker version 2011 (Redmond, WA).

### Western Blot Analysis of Signaling Molecules and Detection of Histones

Whole-cell lysates were prepared by adding Laemmli's sample buffer at  $90^{\circ}\text{C}$  to control or stimulated HDMECs in 12-well dishes and immediately collecting lysates with a cell scraper. Cell lysates were separated on a 7.5% gel by SDS-PAGE and transferred to nitrocellulose membranes. Detection of signaling proteins was performed by

Western blotting with specific primary antibodies and the corresponding horseradish peroxidase-conjugated secondary antibodies. Reactions were detected by chemiluminescence using Immobilon Western horseradish peroxidase substrate (Millipore).

HeH and recombinant PfH3 resuspended in Laemmli's sample buffer were separated on precast 4% to 15% gradient gels (Bio-Rad Laboratories, Mississauga, ON, Canada) by SDS-PAGE. Proteins were visualized by staining with Coomassie Blue. Western blotting of PfH3 was performed with anti-His-probe antibody (1:1000 dilution). Western blots of HeH were probed with BWA3 monoclonal antibody (mAb) for H2A/H4 and LG2-1 for H3 (1  $\mu\text{g}/\text{mL}$  overnight at 4°C with constant agitation).

### Transwell Permeability Assay

A Transwell permeability assay was performed on 12-mm Costar polyester Transwell supports with a pore size of 0.4  $\mu\text{m}$  (Corning Life Sciences, Wilkes Barre, PA), as described previously.<sup>25</sup> Transendothelial resistance (TER) was monitored using an EndOhm voltohmmeter (World Precision Instruments, Sarasota, FL). Permeability was measured with FITC-labeled albumin (250  $\mu\text{g}/\text{mL}$ ), and the amount of leaked labeled albumin was determined by spectrophotometry [Wallac Victor 2 (1420); PerkinElmer, Waltham, MA]. Results are expressed as percent permeability.

### qPCR Array

PCR arrays profiling the expression of 84 pathway-specific genes plus controls (human TLR signaling pathway PCR array; SABiosciences-Qiagen, Frederick, MD) were performed according to the manufacturer's instructions. All PCR array data were analyzed by SuperArray analysis spreadsheet software (SABiosciences), which uses a Student's paired *t*-test based on the corrected  $\Delta\text{C}_T$  values. The  $\Delta\text{C}_T$  values are normalized within each sample by five housekeeping genes:  $\beta$ -2-microglobulin, hypoxanthine phosphoribosyltransferase, ribosomal protein L13a, glyceraldehyde-3-phosphate dehydrogenase, and  $\beta$ -actin.

### qPCR for Human- and Parasite-Derived Genomic DNA

DNA from 400  $\mu\text{L}$  of plasma from patients with acute malaria and controls was extracted using a QIAamp blood kit (Qiagen). qPCR for *P. falciparum* 18S RNA<sup>36</sup> and human  $\beta$ -globin genes<sup>37</sup> was performed by standard methods in an iCycler iQ PCR detection system (Bio-Rad, Copenhagen, Denmark) using SYBR Green dye. The average value of relative cycle number was used to quantify the amount of DNA against a standard curve derived from DNA harvested from IRBCs or HDMECs.

### ELISA for Nucleosome Detection

A cell death detection enzyme-linked immunosorbent assay (ELISA) was performed according to the manufacturer's instructions (ELISA<sup>plus</sup>; Roche Diagnostics, Indianapolis, IN).<sup>38</sup> A standard curve was constructed using purified nucleosomes from *P. yoelii*.<sup>12</sup> Parasite supernatant for detection of nucleosome was generated by culturing 3D7 parasites synchronized with 5% sorbitol within 4 hours of reinvasion. Synchronized IRBCs were cultured in RPMI 1640 + Albumax at 10% parasitemia and 1% hematocrit in six-well plates. One milliliter of culture was collected at 0, 24, 44, 48, 52, 56, and 60 hours. At each time point, the culture supernatant was centrifuged at 2000  $\times g$  for 5 minutes to remove red cells, merozoites, and food vacuoles. The supernatant was stored at -80°C.

### ELISA for Cytokines

Human IL-1 $\beta$ , IL-6, IL-10, IFN- $\gamma$ , and TNF- $\alpha$  expression was determined by an antibody-capture ELISA using an unlabeled anti-human cytokine mAb for capture and a biotinylated mAb for detection (Endogen, Boston, MA), according to the manufacturer's instructions. IL-8 was determined using DuoSet antibodies (R&D Systems). The lower limit of detection of the assays was 15 pg/mL.

### Statistical Analysis

Statistics were performed using GraphPad Prism version 5.00 (GraphPad Software, La Jolla, CA). All *in vitro* data are presented as means  $\pm$  SEM. Data from control and treated cells were compared by Student's *t*-test for paired samples. For multiple comparisons, analysis of variance (analysis of variance) followed by post hoc analysis with Tukey's test was used.  $P \leq 0.05$  was considered statistically significant. For clinical samples, all data were analyzed by nonparametric methods and are reported as median and interquartile ranges.

## Results

### Preparation of *P. falciparum* Histones

*P. falciparum* histones from merozoites were extracted with hydrochloric acid, as described previously.<sup>33</sup> Consistent with previous reports,<sup>33,34</sup> Coomassie Blue staining of the HCl extracts (HeH) separated on a SDS-PAGE gel revealed a number of prominent bands at approximately 10 to 16 kDa, representing histone H2A/B, H3, H4, and their variants (Figure 1A), which together constituted >80% of the total protein content. The specificity of the bands was confirmed by immunoblotting with histone-specific antibodies (Figure 1, B and C). HeH contained minimal double-stranded DNA ( $5.57 \pm 2.49$  ng/50  $\mu\text{g}$  protein). As well, the endotoxin level of the HeH preparations was consistently below the level of detection (<10 pg/5 mg protein).

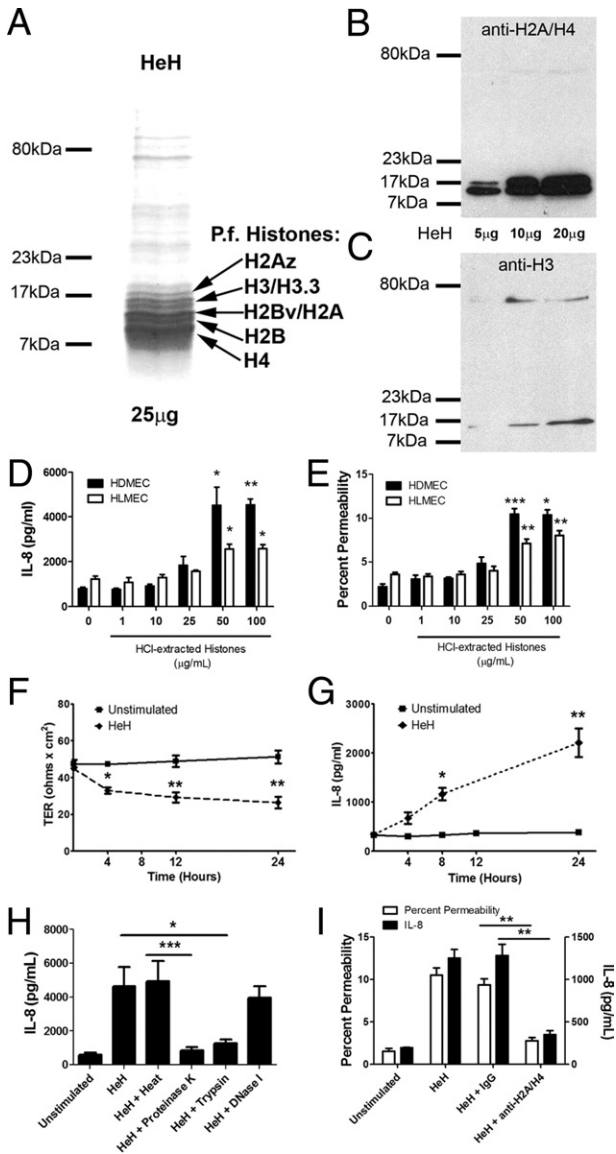


**Figure 1.** *P. falciparum* histone extracts induced IL-8 production and endothelial permeability. **A:** HeH proteins (25  $\mu\text{g}/\text{lane}$ ) from merozoites of parasite clone 3D7 were separated on a 6% SDS-PAGE gel and visualized with Coomassie Blue staining. Prominent bands between 10 and 16 kDa represent H2A/B, H3, H4, and their variants. **A** and **B:** Western blot of HeH probed with 1  $\mu\text{g}/\text{mL}$  of anti-H2A/H4 (BWA3) (**B**) and anti-H3 (LG2-1) (**C**). Results are representative of three different HeH preparations. **D:** Dose-response relationship of HeH for IL-8 production at 24 hours. HDMECs or human lung microvascular endothelial cells (HLMECs) were seeded at  $1 \times 10^4$  cells/well in 96-well plates ( $n = 3$  for each cell type). **E:** Dose-response relationship of HeH for permeability of HDMECs and HLMECs as measured by FITC-albumin flux at 24 hours in a Transwell assay ( $n = 3$  for each cell type). **F:** Time course of HeH on permeability as measured by transendothelial electrical resistance (TER) ( $n = 3$ ). **G:** Time course of HeH on IL-8 production ( $n = 3$ ). **H:** The stimulatory effect of HeH was abrogated by pretreatment with proteinase K and trypsin, but not heat or DNase 1 ( $n = 3$ ). **I:** Inhibition of IL-8 production by histone depletion with mAb BWA3 against H2A/H4 (100  $\mu\text{g}/\text{mL}$ ) ( $n = 3$ ). \* $P < 0.05$ , \*\* $P < 0.01$ , and \*\*\* $P < 0.001$ , compared with control by Student's paired *t*-test, or between indicated groups by analysis of variance with post hoc analysis with Tukey's test.

### *P. falciparum* Histones Induced IL-8 Production and Endothelial Permeability

When HDMECs were stimulated with HeH, IL-8 was induced in a dose-dependent manner (Figure 1D). More-

over, HeH induced gene transcription of a number of other inflammatory mediators involved in proinflammatory signaling pathways, including MCP-1, IL-8, and COX2, but not IFN- $\alpha$  or IFN- $\beta$  (see Supplemental Figure S1 at <http://ajp.amjpathol.org>). HeH also induced an increase in endothelial permeability, as indicated by FITC-albumin flux (Figure 1E) and transendothelial resistance (Figure 1F). Importantly, both IL-8 and permeability responses could be induced in primary human lung microvascular endothelial cells. The effect of HeH on permeability was not significantly different after 4, 12, and 24 hours of stimulation ( $P > 0.05$  for all comparisons) (Figure 1F), whereas IL-8 production continued to increase throughout the 24-hour incubation period (Figure 1G). The activity of HeH was inhibited by proteases, but not by DNase 1 or heat treatment (Figure 1H). Depletion of histone H2A- and H4-containing complexes with mAb BWA3<sup>31</sup> completely removed the activity from HeH (Figure 1I).

These data strongly suggested that histones contribute to the endothelial dysfunction seen in falciparum malaria. To confirm a role for histones, recombinant *P. falciparum* H3 (PfH3) was produced in *E. coli*. The specificity of the recombinant protein was shown by SDS-PAGE gel (Figure 2A) and immunoblotting with anti-H3 antibody (Figure 2B). Because we were unable to obtain a good yield of PfH4, a commercial recombinant human histone H4 was used, which is 92.1% homologous to PfH4 at the amino acid level. Both PfH3 (Figure 2C) and H4 (Figure 2D) induced endothelial permeability and IL-8 at the highest concentration tested (50  $\mu\text{g}/\text{mL}$ ). The recombinant proteins contained <50 pg and <10 pg endotoxin per milligram of protein, respectively. Permeability and IL-8 induced by PfH3 was inhibited by pretreatment of the recombinant histone with proteinase K and the anti-H3 mAb LG2-1,<sup>31</sup> but not polymyxin B, heat, or IgG (Figure 2E). Similar results were obtained with recombinant human histone H4, the activity of which was inhibited by the anti-H2A/H4 mAb BWA3 (Figure 2F).

Based on the observation that histones activate human platelets through TLR2 and TLR4,<sup>39</sup> HDMECs were pretreated with anti-TLR2 (IgG), anti-TLR4 (IgA), or both at 10  $\mu\text{g}/\text{mL}$  before stimulation with HeH. Compared with control IgG, treatment with anti-TLR2 consistently inhibited the IL-8 response to HeH by  $30.1 \pm 2.9\%$  (Figure 3A). On the other hand, anti-TLR4 had a similar inhibitory effect as control IgA, which could be attributed to the negative charge on IgA, which allowed it to bind to positively charged histones.<sup>40</sup> No effect of IgA was seen on the response to lipoteichoic acid or muramyl dipeptide (data not shown). As well, anti-TLR4 but not IgA inhibited the response to ultrapure lipopolysaccharide (100 ng/mL) by >85% (data not shown). Downstream of surface receptors, stimulation with HeH resulted in phosphorylation of Src family kinases (Figure 3B) and p38 MAPK (Figure 3C). IL-8 production was inhibited by pathway-specific inhibitors (Figure 3D). The importance of HeH internalization and subsequent endosomal processing for IL-8 production was demonstrated by pretreatment of HDMECs with chloroquine (25  $\mu\text{mol}/\text{L}$ ), which inhibits endosomal acidification,

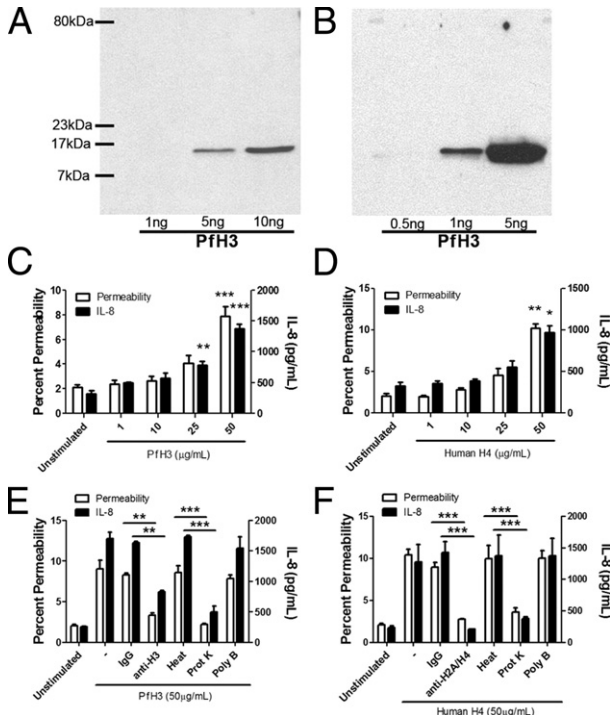


**Figure 2.** Recombinant *P. falciparum* H3 and human H4 induced IL-8 production and endothelial permeability. **A:** Recombinant PfH3 was run on a 6% SDS-PAGE gel and visualized with Coomassie Blue staining. A single band at approximately 15 kDa is seen for both 5 and 10 ng/lane. **B:** Western blot of PfH3 with a polyclonal anti-His tag antibody at 1:1000 dilution. A single band at approximately 15 kDa is seen for both 1 and 5 ng/lane. Results are representative of three independent experiments. **C:** Dose-response relationship of PfH3 for permeability as measured by albumin-FITC flux ( $n = 3$ ) and IL-8 production ( $n = 3$ ) at 24 hours. **D:** Dose-response relationship of human H4 for permeability ( $n = 3$ ) and IL-8 production ( $n = 3$ ) at 24 hours. **E:** Inhibition of permeability and IL-8 production by histone depletion of PfH3 achieved using mAb LG2-1 (100  $\mu\text{g}/\text{mL}$ ) against H3 and proteinase K, but not heat or polymyxin B (20  $\mu\text{g}/\text{mL}$ ) ( $n = 3$ ). **F:** Inhibition of permeability and IL-8 production by histone depletion of human H4 achieved using mAb BWA3 against H2A/H4 (100  $\mu\text{g}/\text{mL}$ ) and proteinase K, but not heat or polymyxin B (20  $\mu\text{g}/\text{mL}$ ) ( $n = 3$ ). \* $P < 0.05$ , \*\* $P < 0.01$ , and \*\*\* $P < 0.001$ , compared with control by Student's paired *t*-test, or between indicated groups by analysis of variance with post hoc analysis with Tukey's test.

and with dynasore (80  $\mu\text{mol}/\text{L}$ ), which inhibits dynamin-mediated endocytosis (Figure 3E).

### Effect of Charge on Endothelial Damage

To determine the mechanism whereby histones induce endothelial permeability, HDMEC monolayers treated with parasite histones were examined under epifluorescence microscopy. As shown previously for cells incubated with parasite merozoites,<sup>25</sup> HeH induced discontinuous staining of the junctional protein ZO-1 and also induced considerable gap formation, compared with untreated controls (Figure 4A). In addition, 39.7  $\pm$  16.7% of cells died when they were stimulated with HeH, compared with 8.4  $\pm$  1.3% of unstimulated cells (Figure 4B). These results are consistent with the cytotoxic effect of calf thymus histones on the endothelial cell line EA.hy96 and primary human umbilical vein endothelial cells.<sup>28</sup> The cytotoxic effect of HeH was not inhibited by the pan-caspase inhibitor Z-VAD-fmk (data not shown), suggest-

ing that cell death was not the result of caspase-dependent apoptosis. In contrast to IL-8 production, induction of permeability did not require p38 MAPK phosphorylation or TLR2 ligation, but was partially Src family kinase-dependent (Figure 4C).

Given that histones are strongly cationic peptides, we next determined whether the observed endothelial damage could be mediated by the positive charge on them. Preincubation of HeH with the polyanionic glucose polymer dextran sulfate abrogated its effect on both endothelial permeability and IL-8 production (Figure 4D). A similar effect was seen with preincubation of HeH with polyanionic polyvinyl sulfate (Figure 4E). The importance of charge for permeability was corroborated by inducing endothelial cell death (Figure 4F) and permeability (Figure 4G) with a positively charged amino acid polymer, poly-L-lysine. However, poly-L-lysine did not induce IL-8 production (Figure 4G), supporting the notion that, although charge appears sufficient for induction of permeability, IL-8 production requires activation of intracellular signaling pathways.

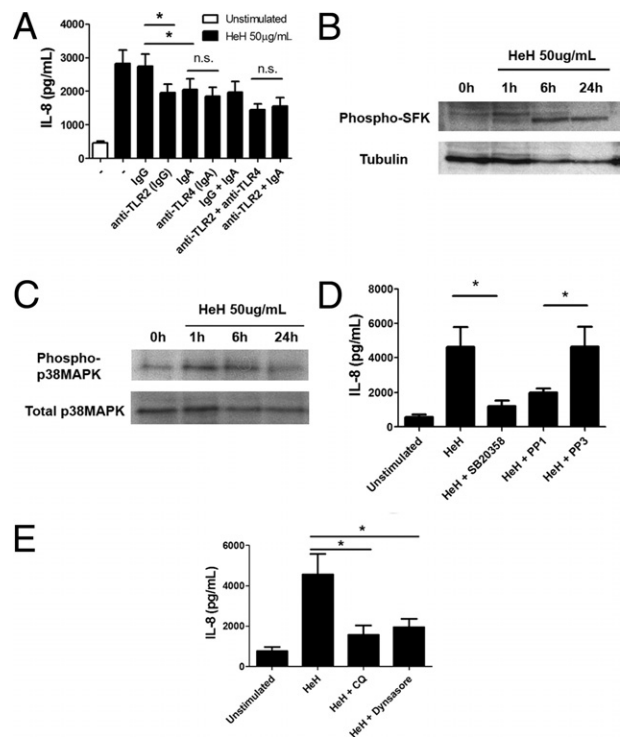


**Figure 3.** *P. falciparum* histone extracts induced IL-8 production through TLR2, Src family kinases, and p38 MAPK. **A:** Partial inhibition of IL-8 production in response to HeH by anti-TLR2, but not anti-TLR4. HDMECs in 96-well plates were preincubated with antibodies (10  $\mu\text{g}/\text{mL}$ ) singly or in combination at 37°C for 30 minutes before the addition of 50  $\mu\text{g}/\text{mL}$  of HeH for 24 hours ( $n = 5$ ). **B:** Time course and Western blot of HeH-induced phosphorylation of Src family kinases. HDMECs were seeded at  $1 \times 10^5$  cells/well in 12-well plates. Lysates at each time point were harvested in 50  $\mu\text{L}$  of hot sample buffer ( $n = 2$ ). **C:** Time course and Western blot of HeH-induced phosphorylation of p38 MAPK ( $n = 2$ ). **D:** Inhibition of IL-8 production in response to HeH by 10  $\mu\text{mol}/\text{L}$  SB20358 and 10  $\mu\text{mol}/\text{L}$  PP1 ( $n = 4$ ). **E:** Inhibition of IL-8 production in response to HeH by chloroquine (25  $\mu\text{mol}/\text{L}$ ) and dynasore (80  $\mu\text{mol}/\text{L}$ ) ( $n = 3$ ). In both **D** and **E**, inhibitors were added 30 minutes before stimulation with HeH. \* $P < 0.05$ , between indicated groups by analysis of variance with post hoc analysis with Tukey's test.

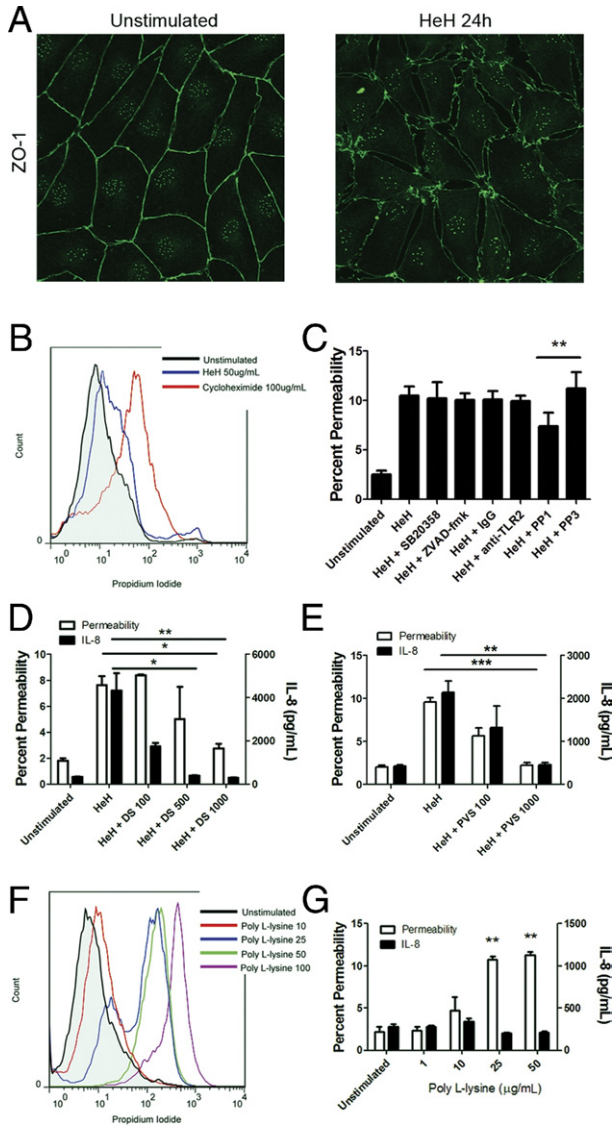


**Figure 4.** Effect of HeH-associated charge on endothelial damage and IL-8 production. **A:**  $1 \times 10^5$  HDMECs were seeded on gelatin-coated glass coverslips and incubated until 3 days after confluence. HeH at  $50 \mu\text{g}/\text{mL}$  was added for 24 hours, after which coverslips were washed in Hank's buffered saline solution and fixed in 1% paraformaldehyde at  $4^\circ\text{C}$  for 30 minutes. Monolayers were stained for ZO-1 expression after permeabilization with 0.1% Triton X-100 and imaged using an Olympus upright IX-81 confocal microscope with a PlanAPO N  $60\times$  NA1.42 objective, argon 488 laser, and Fluoview 1000 software. Compared with unstimulated HDMECs, monolayers stimulated with HeH displayed extensive disruption of paracellular junctions. Results shown are representative of three independent experiments. Original magnification,  $\times 600$ . **B:** Cytotoxicity of HeH on HDMECs as determined by flow cytometry. HDMECs in 96-well plates were incubated with HeH at  $50 \mu\text{g}/\text{mL}$  for 24 hours. Cycloheximide  $100 \mu\text{g}/\text{mL}$  was used as positive control. Cell were trypsinized, washed, and stained with propidium iodide. Results shown are representative of three independent experiments. **C:** Induction of permeability by HeH as measured by FITC-albumin flux in the absence or presence of  $10 \mu\text{mol}/\text{L}$  SB20358 (p38 inhibitor),  $50 \mu\text{M}$  ZVAD-fmk (pan-caspase inhibitor),  $10 \mu\text{mol}/\text{L}$  PP1 (Src family kinase inhibitor), and  $10 \mu\text{mol}/\text{L}$  PP3 (inactive analog) ( $n = 3$ ). **D:** Inhibition of permeability and IL-8 induction when HeH was preincubated with polyanionic dextran sulfate (DS) for 30 minutes at  $37^\circ\text{C}$  ( $n = 3$ ). **E:** Inhibition of permeability and IL-8 induction when HeH was preincubated with polyanionic polyvinyl sulfate (PVS) for 30 minutes at  $37^\circ\text{C}$  ( $n = 3$ ). **F:** Dose-dependent cytotoxicity of poly-L-lysine on HDMECs as determined by propidium iodide uptake ( $n = 3$ ). **G:** Induction of permeability as measured by FITC-albumin flux, but not induction of IL-8 production, was achieved with poly-L-lysine  $25 \mu\text{g}/\text{mL}$  for 24 hours ( $n = 3$ ). \* $P < 0.05$ , \*\* $P < 0.01$ , and \*\*\* $P < 0.001$ , compared with control values by Student's paired *t*-test.

### Activated Protein C Inhibits IL-8 Induction by HeH

Activated protein C is a potent endothelial-derived anti-inflammatory and anti-coagulant factor.<sup>41</sup> The recombinant human protein (rhAPC) is currently in clinical trial for the treatment of sepsis.<sup>42</sup> Among its pleiotropic effects, rhAPC has been shown to protect against endothelial cell death *in vitro*, and against histone-induced mortality in mice *in vivo*, by its proteolytic effect on purified bovine histones.<sup>28</sup> To determine whether rhAPC has a similar proteolytic effect on plasmodial and human histones, PfH3 and human H4 were incubated with  $1 \mu\text{mol}/\text{L}$  rhAPC for 1 hour at  $37^\circ\text{C}$ . Proteolytic cleavage of both recombinant proteins by rhAPC was indicated by the complete loss of the full-size proteins and the associated presence of low molecular weight degradation products (Figure 5A). rhAPC at  $100 \text{ nmol}/\text{L}$  or  $1 \mu\text{mol}/\text{L}$  also cleaved HeH in a time- and dose-dependent manner (Figure 5B). When rhAPC-treated HeH (1 hour at  $37^\circ\text{C}$ ) were added to HDMECs at a final concentration of  $100 \text{ nmol}/\text{L}$  rhAPC and  $50 \mu\text{g}/\text{mL}$  of HeH, IL-8 production was reduced (Figure 5C). On the other hand, inhibition of permeability required preincubation of rhAPC and HeH at  $37^\circ\text{C}$  for 24 hours (Figure 5D). Inactivating rhAPC at the end of the 24 hours of coincubation with HeH by heating the mixture at  $95^\circ\text{C}$  for 15 minutes before addition to HDMECs did not abrogate the inhibitory effect on permeability, suggesting that the action of rhAPC is on histones and not endothelial cells.

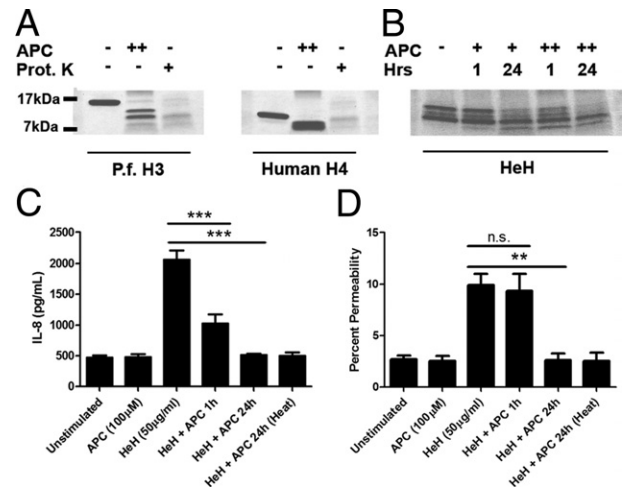


**Figure 5.** Activated protein C inhibited permeability and IL-8 induction by HeH. **A:** Proteolytic degradation of recombinant PfH3 and human H4 by incubation with rhAPC (++,  $1 \mu\text{mol}/\text{L}$ ) or proteinase K (+,  $100 \mu\text{g}/\text{mL}$ ) for 1 hour at  $37^\circ\text{C}$ . Results are representative of two experiments. **B:** Time- and dose-dependent proteolytic degradation of HeH by rhAPC. HeH were incubated with rhAPC (+,  $100 \text{ nmol}/\text{L}$ ; ++,  $1 \mu\text{mol}/\text{L}$ ) for 1 or 24 hours at  $37^\circ\text{C}$ . Gels were stained with Coomassie Blue. Results are representative of two experiments. **C:** Pretreatment of HeH with rhAPC for 1 hour at  $37^\circ\text{C}$  minutes inhibited IL-8 production. Heat inactivation ( $95^\circ\text{C}$  for 10 minutes) of rhAPC + HeH mixture after preincubation for 24 hours but before addition to HDMECs did not abrogate the inhibitory effect of the mixture on IL-8 production ( $n = 3$ ). **D:** Pretreatment of HeH with rhAPC for 24 hours, but not 1 hour, inhibited increase in permeability. Heat inactivation ( $95^\circ\text{C}$  for 10 minutes) of rhAPC + HeH mixture after preincubation for 24 hours but before addition to HDMECs did not abrogate inhibitory effect of the mixture on permeability ( $n = 3$ ). \* $P < 0.05$ , \*\* $P < 0.01$ , and \*\*\* $P < 0.001$  between indicated groups by analysis of variance with post hoc analysis with Tukey's test.

## *P. falciparum* Histones Are Released at Schizogony

To demonstrate that histones could be released during schizogony at the end of the 48-hour life cycle of *P. falciparum*, the release of nuclear contents was examined by live cell imaging. In these experiments, IRBCs containing mature schizonts purified by magnetic-activated cell sorting were observed by confocal microscopy in culture medium containing a membrane impermeable DNA dye, Sytox Green. The Sytox Green signal became strongly positive over the 4 hours after IRBC rupture (Figure 6A). Because Sytox Green is not membrane permeable, the finding indicated either that there was free DNA or that the merozoite membrane had been compromised. At the level of an individual IRBC, the rupture of a merozoite and a schizont occurred over a 10-minute period (Figure 6B; see also Supplemental Video S1 at <http://ajp.amjpathol.org>). We confirmed the release of histones in conjunction with DNA by detecting nucleosomes coincident with IRBC rupture and merozoite release in the supernatant of late-stage schizonts cultured at 10% parasitemia and 1% hematocrit (Figure 6C).

## Circulating Nucleosomes Are Increased in Patients with Severe *Falciparum* Malaria

Induction of endothelial permeability and IL-8 production by parasite histones and the release of parasite histones *in vitro* suggest the potential pathological significance of plasmodial nucleosomes. Nucleosomes are composed of 140 bp of double-stranded DNA wrapped around a protein core of H2A, H2B, H3, and H4 histones. To determine whether these components are present in the circulation during a malarial infection, we used ELISA to measure nucleosome concentrations in plasma samples from a large clinical study on severe falciparum malaria in adults.<sup>29,30</sup> Plasma samples from patients with uncomplicated malaria and sepsis were included for comparison.<sup>43</sup> Nucleosomes were markedly elevated in plasma from patients with severe malaria on admission ( $n = 45$ ), compared with patients with mild infection ( $n = 20$ ) and patients with severe sepsis ( $n = 16$ ) (Figure 7A). There was a significant reduction of circulating nucleosomes in convalescent plasma (7 days after admission), after clearance of infection (Figure 7B). Plasma nucleosome levels correlated significantly with IL-1 $\beta$ , IL-6, IL-8, IL-10, IFN- $\gamma$ , and TNF- $\alpha$  (see Supplemental Figure S2 at <http://ajp.amjpathol.org>). In the small cohort of patients studied, circulating nucleosomes were significantly increased in patients who died of severe falciparum malaria, compared with survivors (Figure 7C).

The significant cytotoxicity of histones on endothelial and perhaps other host cells suggests that circulating nucleosomes in patients could also be of host origin. Indeed, nucleosomes were detected in the culture supernatant of HDMECs stimulated with HeH in a time-dependent manner (Figure 7D). Because the conserved nature of histones precluded determination of the origin of circulating nucleosomes in patients at the protein level, we

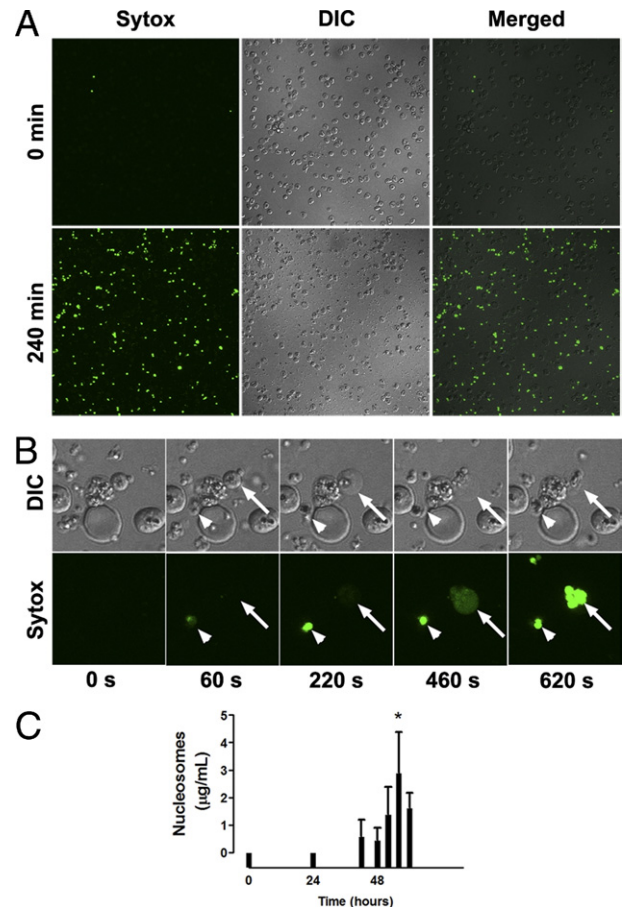


**Figure 6.** Real-time imaging of DNA release at schizogony. Live cell imaging was performed in ibidi  $\mu$ -slide VT<sup>0.4</sup> chambers equilibrated and maintained at 37°C and 5% CO<sub>2</sub> for the duration of the experiment. Purified IRBCs containing late-stage parasites (~46 hours) were added to ibidi chambers precoated with poly-L-lysine (1  $\mu$ mol/L for 10 minutes) to immobilize IRBCs for prolonged imaging. Nonadherent IRBCs were washed off with RPMI 1640, after which RPMI 1640 with 5% Albumax and 300 nmol/L Sytox Green was added to the chambers for the remainder of the experiment. **A:** IRBCs were imaged using an Olympus IX81 inverted confocal microscope with a Plan-APO 60 $\times$  oil immersion objective (NA 1.42), and controlled and captured with FluoView 1000 software. Images were captured before IRBC rupture (0 minutes) and after rupture (240 minutes). No Sytox Green could be detected initially, but after rupture free nuclear materials stained brightly with the membrane-impermeable dye Sytox Green. Differential interference contrast (DIC) images of the same field showing the density of IRBC. Original magnification,  $\times 600$ . **B:** Serial images of the same field of view, digitally magnified  $\times 3.5$ , showing rupture of a schizont (arrow) and a merozoite (arrowhead) over the course of 10 minutes. Still images at 20-second intervals were compiled into a video with NIH ImageJ software version 1.44 (see Supplemental Video S1 at <http://ajp.amjpathol.org>). Results are from one experiment. **C:** Time course of nucleosome release in supernatant of parasite cultures. 3D7 parasites were synchronized with 5% sorbitol within 4 hours of reinvasion. Synchronized IRBCs were cultured in RPMI 1640 + Albumax at 10% parasitemia and 1% hematocrit in six-well plates. Supernatants for nucleosome measurement were collected at 0, 24, 44, 48, 52, 56, and 60 hours ( $n = 3$ ). \* $P < 0.05$ , compared with control values by Student's paired *t*-test.

used qPCR to detect human and parasite DNA in the plasma with primers for *P. falciparum* 18S RNA and human  $\beta$ -globin, as described in *Materials and Methods*. The results showed that, although human DNA was detected in normal controls as well as in patients with uncomplicated falciparum malaria, the level was significantly higher in patients with severe infection (Figure 7E). Parasite DNA was also significantly higher in patients with

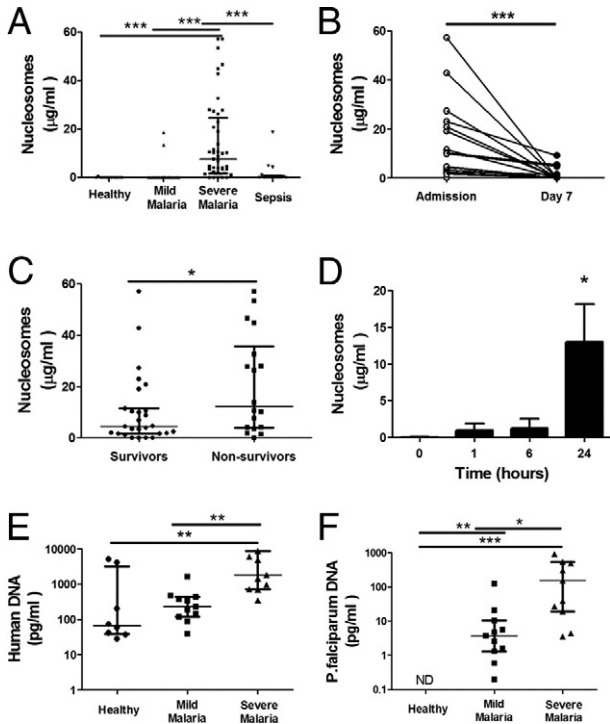


**Figure 7.** Circulating nucleosomes of both human and parasite origin were increased in patients with severe falciparum malaria. Nucleosome levels in plasma from patients with severe and mild falciparum malaria (defined according to World Health Organization criteria) were measured by ELISA. Data are reported as median and interquartile range. **A:** Nucleosome levels at admission were elevated in 45 patients with severe malaria, compared with 20 patients with mild malaria, 13 normal control subjects, and 16 patients with sepsis. **B:** Return of nucleosome levels to normal 7 days after initiation of antimalarial treatment. **C:** Nucleosome levels were higher in nonsurvivors, compared with survivors. **D:** Time course of release of nucleosomes in culture supernatant of HDMECs stimulated with HeH 50 µg/mL. **E:** Quantitation of DNA for the human  $\beta$  globin gene in patient and control plasma ( $n = 11$ ). **F:** Quantitation of DNA for the *P. falciparum* 18S RNA gene in patient and control plasma ( $n = 11$  and 8, respectively). Both host and parasite DNA quantities were higher in patients with severe falciparum malaria. Clinical data were analyzed by nonparametric analysis: Kruskal-Wallis test followed by Dunn's multiple comparison for unmatched multiple comparisons (**A**, **E**, and **F**), Wilcoxon signed rank test for single paired comparisons (**B**), and Mann-Whitney test for single unpaired comparisons (**C**). Data from *in vitro* experiments (**D**) were analyzed by Student's paired *t*-test. \* $P < 0.05$ , \*\* $P < 0.01$ , and \*\*\* $P < 0.001$ .

severe infection (Figure 7F). Taken together with the data from *in vitro* studies, these clinical results suggest that both host and parasite histones could play an important role in endothelial dysfunction and thus outcome of severe falciparum malaria.

### Discussion

Endothelial activation after cocubation with IRBCs has been demonstrated *in vitro* with both primary and immortalized human endothelial cells. The proposed mechanisms of activation (reviewed by Chakravorty et al<sup>44</sup>) are as varied as the cell type or parasite line and assays used. Several studies suggest that, although close proximity of IRBCs to endothelial cells is important for the activation of a proinflammatory response and endothelial permeability, cytoadherence per se may not be crucial.<sup>45–47</sup> Disruption of endothelial junctional proteins could occur as a result of the direct effect of merozoite proteins,<sup>25</sup> or metabolic acidosis induced by IRBCs.<sup>48</sup>

Another report links endothelial permeability to the formation of endothelial cup-like structures at the site of IRBC adhesion.<sup>49</sup> Endothelial cell apoptosis has also been implicated as a mechanism of increased endothelial permeability.<sup>50–52</sup> However, neither apoptosis nor the activation of caspase gene transcription could be confirmed in other studies.<sup>45,46</sup> The one unifying concept that emerges from the disparate results is that modifications of endothelial cells by IRBCs could play a very important role in the outcome of the infection.

The requirement for close proximity of IRBCs and endothelium to elicit endothelial cell activation suggests that some relatively insoluble parasite product may be directly deposited on the endothelium to initiate activation. Candidates include GPI, hemozoin, or products released from food vacuoles or merozoites.<sup>14,25</sup> Activation may be further amplified by exposure to host molecules such as uric acid,<sup>14</sup> phosphatidylserine,<sup>48</sup> or fragments of red cell membrane that have been taken up by trogocytosis.<sup>49</sup> Our results with histones fit well within this paradigm, in that histones are abundant, relatively insoluble proteins released at schizogony and have a strong ability to induce endothelial proinflammatory response, barrier dysfunction, and cell death. The extent of endothelial cytotoxicity *in vivo* remains to be determined. Based on histopathological studies of postmortem tissues, generalized endothelial cell death is not a prominent feature of acute falciparum malaria. However, acute lung injury with associated endothelial cell damage does occur in severe falciparum malaria in adults.<sup>23,24</sup>

Given their strong positive charge, histones may also preferentially accumulate in regions of high negative charge, such as the glomeruli in kidneys, as shown in murine models of lupus nephritis.<sup>53</sup> The high levels of circulating nucleosomes in the plasma of acutely infected patients, compared with what we and others<sup>43</sup> detected in septic patients, and the similarity to cancer patients undergoing chemotherapy for various malignancies<sup>54</sup> suggest that cell death in severe falciparum malaria may be more extensive than previously appreciated. Future studies to clarify a pathogenic role for human and parasite histones *in vivo* should include clinical studies that monitor the time course of release of host and pathogen DNA, as well as the relation to severity. Such studies would be greatly facilitated by antibodies that can discriminate the subtle differences between human and *P. falciparum* histones. Detection of histones in postmortem tissues would also shed light on the *in vivo* distribution of this parasite component.

*P. falciparum* undergoes extensive changes in nucleosome composition during its life cycle.<sup>55</sup> In early rings and in late schizonts/merozoites (ie, at the very beginning and end stages of the erythrocytic 48-hour life cycle), approximately 50% of the genome is found in nucleosomes. *P. falciparum* H3 with the modification H3K9Me1 has been shown to partially colocalize with proteins on the membrane of the parasitophorous vacuole,<sup>56</sup> which suggests that histones may be released from parasitophorous vacuoles or merozoites at the time of schizogony. This result is consistent with what we observed with live cell imaging using Sytox Green and with the detec-

tion of nucleosomes in culture supernatants. Considering that the average parasite burden in a patient with fatal falciparum malaria is approximately  $3.4 \times 10^{12}$ ,<sup>57</sup> and considering that >50% of merozoites do not succeed to reinvade new erythrocytes,<sup>58</sup> the number of extraerythrocytic merozoites that eventually degrade *in vivo* could be considerable, particularly in the microcirculation, where parasitemias are often as high as 100%. That is not even taking into account the amount of host histones that could be released as a consequence of the direct cytotoxic effect of parasite histones.

The strong positive charge (pI ~ 10.5) of histones appeared to be sufficient for the induction of endothelial permeability. Endothelial cells have a negatively charged glycocalyx and basement membrane that is integral to repelling negatively charged albumin (pI ~ 4.5), the primary serum protein responsible for maintenance of fluid balance between the vascular and extravascular compartments. Together with the ability of histones to directly bind albumin, positively charged histones may serve to neutralize these repulsive charge-based forces and allow the flux of albumin across endothelial monolayers, leading to interstitial edema. Histone-induced cell death may also contribute to endothelial permeability. The inability of specific inhibitors of p38 MAPK and caspases to affect permeability, the neutralizing effect of two unrelated polyanionic polymers, and the ability to induce increases in permeability with a polycationic polymer provide further support for a charge-based mechanism of increased permeability by plasmodial histones.

Although *P. falciparum* histones were the subject of the current investigations and clearly have potent proinflammatory and disruptive effects on microvascular endothelium, our results also point to a possible role for host cell-derived histones, which were demonstrated to be released as a result of cell death induced by parasite histones. In addition, there may be other soluble parasite proteins that may be extracted with hydrochloric acid, such as the DNA-binding proteins high mobility group box 1 and 2 (HMGB1 and 2) that, similar to their human counterparts, may activate proinflammatory responses in leukocytes. Human HMGB1, in combination with human or bacterial DNA, has been shown to induce proinflammatory responses in macrophages through activation of TLR2, TLR4, or receptor for advanced glycation end products (RAGE).<sup>59</sup> In endothelial cells, human HMGB1 has been shown to induce permeability through activation of RAGE-dependent<sup>60</sup> and MAPK/PI3K/NF- $\kappa$ B-dependent IL-8, MCP-1, and PAI-1 production.<sup>61</sup> However, unlike the high homology between human and parasite histones, the degree of homology between PfHMGB1 and PfHMGB2 and the human proteins is low (23% and 21%, respectively). Plasmodia also possess heat shock proteins (HSP), and PfHSP70 is thought to have adjuvant and proinflammatory activities through TLR2/4 and TLR4/MyD88 activation, respectively.<sup>62</sup> Future studies of the effect of these and other potential mediators in endothelial cells may shed new light on the pathogenic role of additional subcellular parasite components.

As reported previously for calf thymus histones,<sup>28</sup> the protective effect of rhAPC against plasmodial histones

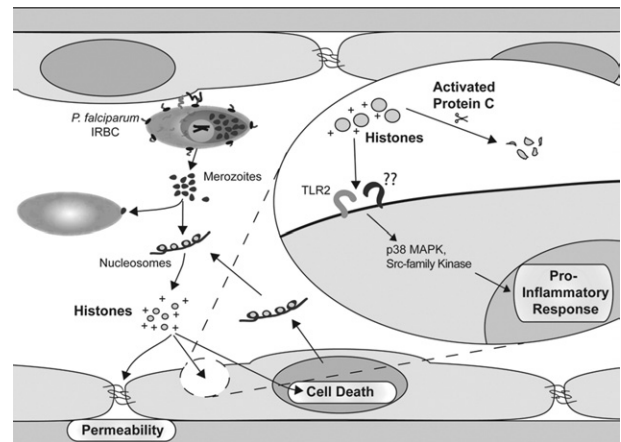


**Figure 8.** Proposed model of the induction of endothelial proinflammatory response and barrier dysfunction by *P. falciparum* histones. Parasite histones from merozoites are released in the proximity of endothelial cells during schizogony of cytoadherent IRBCs, where they exert a disruptive effect on endothelial barrier function through a charge-related mechanism. In addition, parasite histones activate TLR2 and other innate receptors, leading to the induction of inflammatory mediators through a signaling pathway involving the Src family kinases and p38 MAPK. The pathological effect of parasite histones may be further amplified by the release of host histones and other endogenous mediators from dying cells. The proinflammatory activity of both plasmodial and human histones can be inhibited by rhAPC.

appeared to be related to its dose- and time-dependent proteolytic activity. The longer preincubation of rhAPC with HeH required for the inhibition of permeability, compared with inhibition of IL-8 production, could be due to the fact that permeability reached maximum levels earlier (<4 hours) than did IL-8 ( $\geq 24$  hours), so that histones needed to be sufficiently degraded before addition to endothelial cells. The concentration of rhAPC required to degrade plasmodium histones *in vitro* was 2 to 3 log higher than the reported mean steady-state circulating rhAPC level of 50 ng/mL, achieved in patients given the standard infusion of 24  $\mu$ g/kg/h for 96 hours.<sup>63</sup> Nevertheless, degraded histones were detected in the plasma of a patient with sepsis who received rhAPC, and physiological doses of rhAPC are proteolytic toward histones when potentiated by lipids found in serum.<sup>28</sup> In addition to its activity on histones, rhAPC may be beneficial in select patients with severe falciparum malaria through its pleiotropic effects on coagulation, inflammation, and permeability (reviewed by Mosnier et al<sup>41</sup>). Clinical improvement within hours of rhAPC administration has been described in three separate case reports of severe malaria.<sup>64–66</sup>

In conclusion, our results provide significant new insight into endothelial activation in *P. falciparum* malaria by identifying histones of both human and parasite origin as strong inducers of a complex pattern of endothelial cell responses (Figure 8). We propose that parasite histones from merozoites released in the proximity of endothelial cells during schizogony of cytoadherent IRBCs exert a disruptive effect on endothelial barrier function through a charge-related mechanism. In addition, parasite histones activate TLR2 and other innate receptors, leading to the induction of inflammatory mediators through a signaling pathway involving Src family kinases and p38 MAPK. The pathological effect of parasite histones may be further

amplified by the release of host histones and other endogenous mediators from dying cells. The proinflammatory activity of both plasmodial and human histones can be inhibited by rhAPC. These results may have important implications for infection with other histone-containing pathogens, such as parasites and fungi. We have also identified possible new targets for therapeutic interventions in severe falciparum malaria, including halting endothelial activation by using rhAPC.

### Acknowledgments

We thank Dr. Carolyn Lane (Valley View Family Practice Clinic, Calgary, AB, Canada) for providing skin specimens and Dr. Bryan Yipp (Foothills Hospital, Calgary, AB, Canada) for providing serum samples from patients with sepsis.

### References

1. Maier AG, Cooke BM, Cowman AF, Tilley L: Malaria parasite proteins that remodel the host erythrocyte. *Nat Rev Microbiol* 2009, 7:341–354
2. Ho M, White NJ: Molecular mechanisms of cytoadherence in malaria. *Am J Physiol* 1999, 276:C1231–C1242
3. Bate CA, Taverne J, Bootsma HJ, Mason RC, Skalko N, Gregoriadis G, Playfair JH: Antibodies against phosphatidylinositol and inositol monophosphate specifically inhibit tumour necrosis factor induction by malaria exoantigens. *Immunology* 1992, 76:35–41
4. Schofield L, Hackett F: Signal transduction in host cells by a glycosylphosphatidylinositol toxin of malaria parasites. *J Exp Med* 1993, 177:145–153
5. Krishnegowda G, Hajjar AM, Zhu J, Douglass EJ, Uematsu S, Akira S, Woods AS, Gowda DC: Induction of proinflammatory responses in macrophages by the glycosylphosphatidylinositols of *Plasmodium falciparum*: cell signaling receptors, glycosylphosphatidylinositol (GPI) structural requirement, and regulation of GPI activity. *J Biol Chem* 2005, 280:8606–8616
6. Zhu J, Krishnegowda G, Gowda DC: Induction of proinflammatory responses in macrophages by the glycosylphosphatidylinositols of *Plasmodium falciparum*: the requirement of extracellular signal-regulated kinase, p38, c-Jun N-terminal kinase and NF-kappaB pathways for the expression of proinflammatory cytokines and nitric oxide. *J Biol Chem* 2005, 280:8617–8627
7. Shio MT, Eisenbarth SC, Savaria M, Vinet AF, Bellemare MJ, Harder KW, Sutterwala FS, Bohle DS, Descoteaux A, Flavell RA, Olivier M: Malarial hemozoin activates the NLRP3 inflammasome through Lyn and Syk kinases. *PLoS Pathog* 2009, 5:e1000559
8. Dostert C, Guarda G, Romero JF, Menu P, Gross O, Tardivel A, Suva ML, Stehle JC, Kopf M, Stamenkovic I, Corradin G, Tschopp J: Malarial hemozoin is a Nalp3 inflammasome activating danger signal. *PLoS One* 2009, 4:e6510
9. Reimer T, Shaw MH, Franchi L, Coban C, Ishii KJ, Akira S, Horii T, Rodriguez A, Núñez G: Experimental cerebral malaria progresses independently of the Nlrp3 inflammasome. *Eur J Immunol* 2010, 40:764–769
10. Parroche P, Lauw FN, Goutagny N, Latz E, Monks BG, Visintin A, Halmen KA, Lamphier M, Olivier M, Bartholomeu DC, Gazzinelli RT, Golenbock DT: Malaria hemozoin is immunologically inert but radically enhances innate responses by presenting malaria DNA to Toll-like receptor 9. *Proc Natl Acad Sci USA* 2007, 104:1919–1924
11. Coban C, Ishii KJ, Kawai T, Hemmi H, Sato S, Uematsu S, Yamamoto M, Takeuchi O, Itagaki S, Kumar N, Horii T, Akira S: Toll-like receptor 9 mediates innate immune activation by the malaria pigment hemozoin. *J Exp Med* 2005, 201:19–25
12. Gowda NM, Wu X, Gowda DC: The nucleosome (histone-DNA complex) is the TLR9-specific immunostimulatory component of *Plasmodium falciparum* that activates DCs. *PLoS One* 6:e20398
13. Lande R, Gregorio J, Facchinetti V, Chatterjee B, Wang YH, Homey B, Cao W, Su B, Nestle FO, Zal T, Mellman I, Schroder JM, Liu YJ, Gillie

- M: Plasmacytoid dendritic cells sense self-DNA coupled with antimicrobial peptide. *Nature* 2007, 449:564–569
14. Griffith JW, Sun T, McIntosh MT, Bucala R: Pure Hemozoin is inflammatory in vivo and activates the NALP3 inflammasome via release of uric acid. *J Immunol* 2009, 183:5208–5220
15. Martinon F, Pétrilli V, Mayor A, Tardivel A, Tschopp J: Gout-associated uric acid crystals activate the NALP3 inflammasome. *Nature* 2006, 440:237–241
16. Orengo JM, Evans JE, Bettiol E, Leliwa-Sytek A, Day K, Rodriguez A: Plasmodium-induced inflammation by uric acid. *PLoS Pathog* 2008, 4:e1000013
17. Ye X, Ding J, Zhou X, Chen G, Liu SF: Divergent roles of endothelial NF-kappaB in multiple organ injury and bacterial clearance in mouse models of sepsis [Erratum appeared in *J Exp Med* 2008;205:1509]. *J Exp Med* 2008, 205:1303–1315
18. Andonegui G, Zhou H, Bullard D, Kelly MM, Mullaly SC, McDonald B, Long EM, Robbins SM, Kubes P: Mice that exclusively express TLR4 on endothelial cells can efficiently clear a lethal systemic Gram-negative bacterial infection. *J Clin Invest* 2009, 119:1921–1930
19. Gillrie MR, Zbytniuk L, McAvoy E, Kapadia R, Lee K, Waterhouse CC, Davis SP, Muruve DA, Kubes P, Ho M: Divergent roles of Toll-like receptor 2 in response to lipoteichoic acid and *Staphylococcus aureus* in vivo. *Eur J Immunol* 2010, 40:1639–1650
20. Turner GD, Ly VC, Nguyen TH, Tran TH, Nguyen HP, Bethell D, Wyllie S, Louwrier K, Fox SB, Gatter KC, Day NP, White NJ, Berendt AR: Systemic endothelial activation occurs in both mild and severe malaria. Correlating dermal microvascular endothelial cell phenotype and soluble cell adhesion molecules with disease severity. *Am J Pathol* 1998, 152:1477–1487
21. Brown H, Turner G, Rogerson S, Tembo M, Mwenechanya J, Molyneux M, Taylor T: Cytokine expression in the brain in human cerebral malaria. *J Infect Dis* 1999, 180:1742–1746
22. Brown H, Rogerson S, Taylor T, Tembo M, Mwenechanya J, Molyneux M, Turner G: Blood-brain barrier function in cerebral malaria in Malawian children. *Am J Trop Med Hyg* 2001, 64:207–213
23. Brooks MH, Kiel FW, Sheehy TW, Barry KG: Acute pulmonary edema in falciparum malaria: a clinicopathological correlation. *N Engl J Med* 1968, 279:732–737
24. Maguire GP, Handoyo T, Pain MC, Kenangalem E, Price RN, Tjitra E, Anstey NM: Lung injury in uncomplicated and severe falciparum malaria: a longitudinal study in Papua, Indonesia. *J Infect Dis* 2005, 192:1966–1974
25. Gillrie MR, Krishnegowda G, Lee K, Buret AG, Robbins SM, Looareesuwan S, Gowda DC, Ho M: Src-family kinase dependent disruption of endothelial barrier function by *Plasmodium falciparum* merozoite proteins. *Blood* 2007, 110:3426–3435
26. Hirsch JG: Bactericidal action of histone. *J Exp Med* 1958, 108:925–944
27. Brinkmann V, Reichard U, Goosmann C, Fauler B, Uhlemann Y, Weiss DS, Weinrauch Y, Zychlinsky A: Neutrophil extracellular traps kill bacteria. *Science* 2004, 303:1532–1535
28. Xu J, Zhang X, Pelayo R, Monestier M, Ammollo CT, Semeraro F, Taylor FB, Esmon NL, Lupu F, Esmon CT: Extracellular histones are major mediators of death in sepsis. *Nat Med* 2009, 15:1318–1321
29. Day NP, Hien TT, Schollaardt T, Loc PP, Chuong LV, Chau TT, Mai NT, Phu NH, Sinh DX, White NJ, Ho M: The prognostic and pathophysiological role of pro- and antiinflammatory cytokines in severe malaria. *J Infect Dis* 1999, 180:1288–1297
30. Tran TH, Day NP, Nguyen HP, Nguyen TH, Pham PL, Dinh XS, Ly VC, Ha V, Waller D, Peto TE, White NJ: A controlled trial of artemether or quinine in Vietnamese adults with severe falciparum malaria. *N Engl J Med* 1996, 335:76–83
31. Monestier M, Fasy TM, Losman MJ, Novick KE, Muller S: Structure and binding properties of monoclonal antibodies to core histones from autoimmune mice. *Mol Immunol* 1993, 30:1069–1075
32. Yipp BG, Anand S, Schollaardt T, Patel KD, Looareesuwan S, Ho M: Synergism of multiple adhesion molecules in mediating cytoadherence of *Plasmodium falciparum*-infected erythrocytes to microvascular endothelial cells under flow. *Blood* 2000, 96:2292–2298
33. Longhurst HJ, Holder AA: The histones of *Plasmodium falciparum*: identification, purification and a possible role in the pathology of malaria. *Parasitology* 1997, 114 (Pt 5):413–419

34. Miao J, Fan Q, Cui L, Li J, Li J, Cui L: The malaria parasite *Plasmodium falciparum* histones: organization, expression, and acetylation. *Gene* 2006, 369:53–65
35. Ribaut C, Berry A, Chevalley S, Reybier K, Morlais I, Parzy D, Nepveu F, Benoit-Vical F, Valentin A: Concentration and purification by magnetic separation of the erythrocytic stages of all human *Plasmodium* species. *Malar J* 2008, 7:45
36. Nwakanma DC, Gomez-Escobar N, Walther M, Crozier S, Dubovsky F, Malkin E, Locke E, Conway DJ: Quantitative detection of *Plasmodium falciparum* DNA in saliva, blood, and urine. *J Infect Dis* 2009, 199:1567–1574
37. Lo YM, Tein MS, Lau TK, Haines CJ, Leung TN, Poon PM, Wainscoat JS, Johnson PJ, Chang AM, Hjelm NM: Quantitative analysis of fetal DNA in maternal plasma and serum: implications for noninvasive prenatal diagnosis. *Am J Hum Genet* 1998, 62:768–775
38. Holdenrieder S, Stieber P, Bodenmüller H, Fertig G, Fürst H, Schmeller N, Untch M, Seidel D: Nucleosomes in serum as a marker for cell death. *Clin Chem Lab Med* 2001, 39:596–605
39. Semeraro F, Ammolto CT, Morrissey JH, Dale GL, Friese P, Esmon NL, Esmon CT: Extracellular histones promote thrombin generation through platelet-dependent mechanisms: involvement of platelet TLR2 and TLR4. *Blood* 118:1952–1961
40. Chiodi F, Sidén ÅA, Ösby E: Isoelectric focusing of monoclonal immunoglobulin G<sub>1</sub> A and M followed by detection with the avidin-biotin system. *Electrophoresis* 1985, 6:124–128
41. Mosnier LO, Zlokovic BV, Griffin JH: The cytoprotective protein C pathway. *Blood* 2007, 109:3161–3172
42. Bernard GR, Vincent JL, Laterre PF, LaRosa SP, Dhainaut JF, Lopez-Rodriguez A, Steingrub JS, Garber GE, Helterbrand JD, Ely EW, Fisher CJ Jr; Recombinant Human Protein C Worldwide Evaluation in Severe Sepsis (PROWESS) Study Group: Efficacy and safety of recombinant human activated protein C for severe sepsis. *N Engl J Med* 2001, 344:699–709
43. Zeerleder S, Zwart B, Willemin WA, Aarden LA, Groeneveld AB, Caliezi C, van Nieuwenhuijze AE, van Mierlo GJ, Eerenberg AJ, Lämmle B, Hack CE: Elevated nucleosome levels in systemic inflammation and sepsis. *Crit Care Med* 2003, 31:1947–1951
44. Chakravorty SJ, Hughes KR, Craig AG: Host response to cytoadherence in *Plasmodium falciparum*. *Biochem Soc Trans* 2008, 36:221–228
45. Tripathi AK, Sullivan DJ, Stins MF: *Plasmodium falciparum*-infected erythrocytes decrease the integrity of human blood-brain barrier endothelial cell monolayers. *J Infect Dis* 2007, 195:942–950
46. Chakravorty SJ, Carret C, Nash GB, Ivens A, Szeszak T, Craig AG: Altered phenotype and gene transcription in endothelial cells, induced by *Plasmodium falciparum*-infected red blood cells: pathogenic or protective? *Int J Parasitol* 2007, 37:975–987
47. Tripathi AK, Sha W, Shulaev V, Stins MF, Sullivan DJ Jr: *Plasmodium falciparum*-infected erythrocytes induce NF- $\kappa$ B regulated inflammatory pathways in human cerebral endothelium. *Blood* 2009, 114:4243–4252
48. Zougbedé S, Miller F, Ravassard P, Rebollo A, Cicéron L, Couraud PO, Mazier D, Moreno A: Metabolic acidosis induced by *Plasmodium falciparum* intraerythrocytic stages alters blood-brain barrier integrity. *J Cereb Blood Flow Metab* 2011, 31:514–526
49. Jambou R, Combes V, Jambou MJ, Weksler BB, Couraud PO, Grau GE: *Plasmodium falciparum* adhesion on human brain microvascular endothelial cells involves transmigration-like cup formation and induces opening of intercellular junctions. *PLoS Pathog* 2010, 6:e1001021
50. Pino P, Vouldoukis I, Kolb JP, Mahmoudi N, Desportes-Livage I, Bricaire F, Danis M, Dugas B, Mazier D: *Plasmodium falciparum*-infected erythrocyte adhesion induces caspase activation and apoptosis in human endothelial cells. *J Infect Dis* 2003, 187:1283–1290
51. Taoufiq Z, Gay F, Balvanos J, Ciceron L, Tefit M, Lechat P, Mazier D: Rho kinase inhibition in severe malaria: thwarting parasite-induced collateral damage to endothelia. *J Infect Dis* 2008, 197:1062–1073
52. Wilson NO, Huang MB, Anderson W, Bond V, Powell M, Thompson WE, Armah HB, Adjei AA, Gyasi R, Tettey Y, Stiles JK: Soluble factors from *Plasmodium falciparum*-infected erythrocytes induce apoptosis in human brain vascular endothelial and neuroglia cells. *Mol Biochem Parasitol* 2008, 162:172–176
53. Schmiedeke T, Stoeckl F, Muller S, Sugisaki Y, Batsford S, Woitas R, Vogt A: Glomerular immune deposits in murine lupus models may contain histones. *Clin Exp Immunol* 1992, 90:453–458
54. Holdenrieder S, Stieber P, Bodenmüller H, Busch M, Fertig G, Fürst H, Schalhorn A, Schmeller N, Untch M, Seidel D: Nucleosomes in serum of patients with benign and malignant diseases [Erratum appeared in *Int J Cancer* 2001, 95:398]. *Int J Cancer* 2001, 95:114–120
55. Ponts N, Harris EY, Prudhomme J, Wick I, Eckhardt-Ludka C, Hicks GR, Hardiman G, Lonardi S, Le Roch KG: Nucleosome landscape and control of transcription in the human malaria parasite. *Genome Res* 2010, 20:228–238
56. Luah YH, Chaal BK, Ong EZ, Bozdech Z: A moonlighting function of *Plasmodium falciparum* histone 3, mono-methylated at lysine 9? *PLoS One* 2010, 5:e10252
57. Dondorp AM, Desakorn V, Pongtavornpinyo W, Sahassananda D, Silamut K, Chotivanich K, Newton PN, Pitisuttithum P, Smithyman AM, White NJ, Day NP: Estimation of the total parasite biomass in acute *falciparum* malaria from plasma PfHRP2 [Erratum appeared in *PLoS Med* 2005;2:390]. *PLoS Med* 2005, 2:e204
58. White NJ, Chapman D, Watt G: The effects of multiplication and synchronicity on the vascular distribution of parasites in *falciparum* malaria. *Trans R Soc Trop Med Hyg* 1992, 86:590–597
59. Sims GP, Rowe DC, Rietdijk ST, Herbst R, Coyle AJ: HMGB1 and RAGE in inflammation and cancer. *Annu Rev Immunol* 2010, 28:367–388
60. Wolfson RK, Chiang ET, Garcia JG: HMGB1 induces human lung endothelial cell cytoskeletal rearrangement and barrier disruption. *Microvasc Res* 2011, 81:189–197
61. Fiuzza C, Bustin M, Talwar S, Tropea M, Gerstenberger E, Shelhamer JH, Suffredini AF: Inflammation-promoting activity of HMGB1 on human microvascular endothelial cells. *Blood* 2003, 101:2652–2660
62. Kumar K, Singal A, Rizvi MM, Chauhan VS: High mobility group box (HMGB) proteins of *Plasmodium falciparum*: DNA binding proteins with pro-inflammatory activity. *Parasitol Int* 2008, 57:150–157
63. Macias WL, Dhainaut JF, Yan SC, Helterbrand JD, Seger M, Johnson G 3rd, Small DS: Pharmacokinetic-pharmacodynamic analysis of drotrecogin alfa (activated) in patients with severe sepsis. *Clin Pharmacol Ther* 2002, 72:391–402
64. Robak O, Bojic A, Locker GJ, Laczika K, Ramharter M, Staudinger T: The use of drotrecogin alfa in severe *falciparum* malaria. *Anaesth Intensive Care* 2010, 38:751–754
65. Kendrick BJ, Gray AG, Pickworth A, Watters MP: Drotrecogin alfa (activated) in severe *falciparum* malaria. *Anaesthesia* 2006, 61:899–902
66. Rankin LG, Austin DL: The use of activated protein C in severe *Plasmodium falciparum* malaria. *Anaesth Intensive Care* 2007, 35:428–432